MODELING THE EFFECTS OF DUST SIZE DISTRIBUTION, COMPOSITION, AND CHARGING PHYSICS ON THE ELECTRIC ENVIRONMENT OF MARTIAN DUST DEVILS

E. L. Barth, *Southwest Research Institute, Boulder, CO, USA (ebarth@boulder.swri.edu)*, **W. M. Farrell**, *Solar System Exploration Division, NASA/Goddard Space Flight Center, Greenbelt,* **S. C. R. Rafkin**, *Southwest Research Institute, Boulder, CO, USA.*

Introduction: While Martian dust devils have been monitored through decades of observations, we have yet to study their possible electrical effects from *in situ* instrumentation. However, evidence for the existence of active electrodynamic processes on Mars is provided by laboratory studies of analog material and field campaigns of dust devils on Earth. Dust charging studies using Mars soil simulant (Krauss et al., 2003; Sternovsky et al., 2002) suggest that the charged dust observed within terrestrial dust disturbances (*e.g.* Farrell et al., 2004; Renno et al., 2004) is very possible on Mars.

Electric fields measured in the vicinity of terrestrial dust devils are the result of triboelectric charging of individual dust grains, most of which occurs in the saltation layer within the first few centimeters of the surface. Once charged, some of these grains are injected further into the air where they are transported upward by atmospheric currents. Differential transport and gravitational sedimentation sorts the dust devil aerosols by size so that the smaller and predominantly negatively charged particles populate the higher portion of the disturbance while the larger, positively charged particles fall to the ground or remain in the lower portion of the vortex.

The vertical velocities within Martian dust devils can lift the charged dust particles, the smallest particles, hundreds of meters or more above the surface in a coherent column creating a charge separation that may be large enough to produce significant electric fields. On Mars, electric fields are limited by large increases in atmospheric conductivity when they reach sufficient magnitude to ionize CO_2 and by electric discharges thought to occur at ~20 to 25 kV/m (Kok and Renno 2009).

Consideration of electrodynamical processes is significant for numerous reasons. First, electrodynamical processes are implicated in the local production of superoxides at concentrations orders of magnitude greater than expected through photochemistry, and are further implicated in the subsequent destruction of organics. Second, there are potential hazards associated with an active electromagnetic environment, including electrical discharges and communication disruption. And third, naturally occurring electromagnetic fields can be used to passively probe orders of magnitude deeper into the interior of Mars than is possible with conventional ground penetrating radars. However, to characterize the magnitude of each of the above issues, basic and fundamental knowledge of the electrodynamic environment first must be established. Modeling work is currently the only practical way to constrain Mars' electrodynamic environment.

We have integrated the dust devil dynamics studies of Michaels and Rafkin 2004 with the particle charging of Farrell et al. 2006 to create a model which can explore the charge environment throughout the lifecycle of a dust devil. Specifically, we have modified the Mars Regional Atmospheric Modeling System (MRAMS) to include charge distribution as a function of dust particle size and composition, provided by the Macroscopic Triboelectric Simulation (MTS) code.

Modeling: MRAMS is used to investigate the complex physics of regional, mesoscale, and microscale atmospheric phenomena on Mars (*e.g.* Rafkin et al. 2001). It is a 3-D, nonhydrostatic model, which permits the simulation of atmospheric flows with large vertical accelerations, such as dust devils (Michaels 2006).

Our simulations described here have been initialized homogeneously using temperature and wind profiles from a Viking 1 landing site mesoscale simulation (Fenton and Michaels 2010) at approximately 10:00 LMST (local mean solar time). We run the model over a 15 km x 15 km x 7 km grid with 100 m grid-spacing in x and y and a vertical grid that stretches with height, starting from a layer thickness of 4 m near the surface to a layer thickness of 150 m at the top (150 x 150 x 64 grid points).

MRAMS includes a number of microphysics routines which simulate the transport and microphysical interactions of dust aerosols. Dust sources are provided via a surface dust lifting scheme, and the sink of dust is sedimentation to the surface. The dust lifting scheme includes multi-size dust transport capability (Michaels 2006). The dust surface source is parameterized based on the work of Armstrong and Leovy 2005.

MTS is a 3-D particle code which quantifies charging associated with swirling, mixing dust grains (Farrell et al. 2003; Farrell et al. 2006). Grains of pre-defined sizes and compositions are placed in a simulation box and allowed to move under the influence of winds and gravity. The model tracks the movement of individual grains in prevailing (cyclostrophic) winds and charge exchange upon grain-

grain collision.

We impose a compositional mix to maximize the triboelectric surface potential difference ($\Delta\Phi$) between larger and smaller grains. Specifically, we apply the grain-grain contact electrification algorithm presented in Desch and Cuzzi 2000. As a rule, we use $\Delta\Phi$ = 1.6 V to simulate a mixture of smaller metallic and larger basaltic type particles. We also consider cases where we treat $\Delta\Phi$ as a free parameter by examining the degree of electrification and grain charge-size distribution for a range of values approaching zero (uniform composition).

Information describing each MTS dust particle (*i.e.,* charge, radius, and mass) is used to instruct the MRAMS dust lifting scheme for each MRAMS model grid-cell. The amount of charge on the MTS dust grains reflects the point where the dust grain movement has become non-collisional and so there is no longer charge exchange through grain-grain collision.

The MTS dust grain information is binned into the appropriate microphysics mass/radius bins (Fig. 1, top panel). A lognormal function is then fit to the charge profile (Fig. 1, bottom panel). The first and second moments of the charge distribution are implemented as dynamical tracers within MRAMS so that as the dust moves within the MRAMS domain, the charge distribution can be reconstructed for any grid point. The distribution of charge in an MRAMS grid box will change as the size distribution of particles evolves due to the effects of winds and gravity. MRAMS keeps track of the charge density as a passive tracer. This can then be used to calculate an electric field from the Poisson equation.

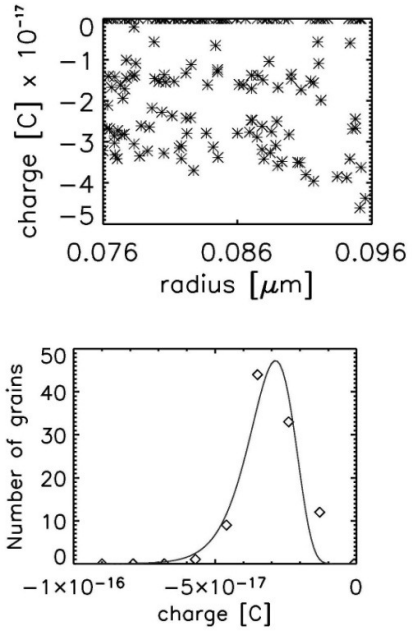

Figure 1. The top panel shows the raw output from MTS with the charge on each individual dust grain within in a given size range dictated by MRAMS. This information is used by MRAMS to bin the charge as shown in the bottomt panel. The charge distribution can be approximated by a log-normal distribution. MRAMS dynamic tracers are then (1) total particle number, (2) number of neutrals, (3) charge distribution first moment, and (4) charge distribution second moment.

Dust Devil Simulation Results: Barth et al. (2015) found that electric fields are generated everywhere dust lifting occurs. The electric fields generated within the dust devils vary in strength due to three main factors: size of the dust particles, average charge density, and the number of dust particles in the atmosphere (controlled by the parameterized dust lifting efficiency). To isolate the effects of each of the variable parameters (size, charge, lifting), six cases were run and the results compared by looking at electric fields produced by the same dust devil in each model run. These cases are summarized in Table 1.

Table 1. Summary of dust devil sensitivity tests (in order of increasing electric field).

	Radius	Charge	Lifting eff.	Number* (cm^{-3})	Optical depth**	E-field* (V/m)
A	Small	Small	9e-8	11	5e-3	0.11
D	Small	Small	9e-7	110	5e-2	1.6
E	Small	Large	9e-8	16	5e-3	4.5
C	Large	large	9e-5	16	5e-1	39
F	large	small	9e-3	1100	5	200
B	large	large	9e-3	1600	50	3900

*Corresponding to maximum contour level in the plane 2 m above the surface

**Estimated visible-wavelength horizontal optical depth of the dust devil column

The dust particle size distributions were based on a known published distribution from Farrell et al. 2006 that possesses an adjustable power law particle size distribution. This power law type distribution was similar in nature to that used by Melnik and Parrot 1998. The dust particles are classified as either metals or basalts based on their charge sign (negative or positive, respectively). In the *small radius* case, the metals range from 0.05 – 0.2 μm in radius, with most particles having a radius of 0.1 μm; the basaltic particles are 0.2 – 10 μm in radius, with the peak of the size distribution at ~0.4 μm. Because the basalts are much less dense than the metals, the smaller basaltic particles fall at speeds comparable to the metal particles. Scaling both of the size distributions up by a factor of 10 (the *large radius* case) results in a greater vertical separation between the two populations of particles within a dust devil.

The charge on individual particles ranges from about 10^{-18} to 10^{-15} C. A number of neutral particles

are also present. Figure 2 shows the average charge density distributions.

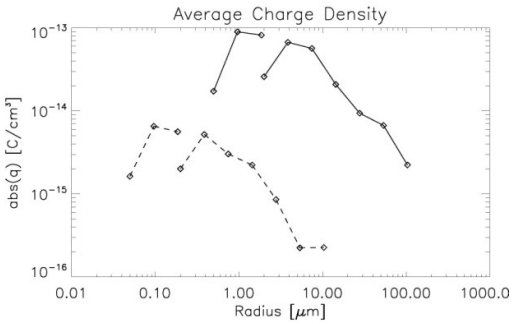

Figure 2. Average charge density distributions applied to the two size distribution cases described above. Absolute value is shown for the negatively charged particles.

The dust lifting efficiency regulates the amount of mass lifted and so controls the number of dust particles lifted into the atmosphere. The numerical value is specific to the dust lifting parameterization in the model (numerical values are listed in Table 1 to illustrate the difference between the cases; a more physical way to distinguish between the cases is to look at the number of particles in the dust devils).

Given the estimated visible-wavelength horizontal optical depth of the dust devil column, Case C might be a reasonable representation of Martian dust devils a few 100 m in diameter. Figure 3 shows the modeled electric field environment. The maximum electric fields are ~ 40 V/m.

We expand upon our previous studies here in order to (1) determine the influence of the lifted dust size distribution and dust composition on the electromagnetic environment, and (2) compare the modeling results obtained by assuming each of the triboelectric charging physics proposed by Desch and Cuzzi (2000), Melnik and Parrot (1998), Kok and Renno (2009), and Forward et al. (2009).

The properties of surface dust likely vary from place to place on Mars. There are certainly regions of high dust availability and other regions where available dust is low either due to the absence or the immobilization (e.g. via cementation) of such particles. The size distribution of available dust almost certainly varies as well. Finally, the composition of the dust (particularly the larger particles) may vary across Mars. These factors affect the electric potential of the dust and potentially the resultant charging.

Desch and Cuzzi include dust composition effects in addition to size in their triboelectric charging physics. Melnik and Parrot use only size as a dependent parameter for charging. Kok and Renno describe a new set of empirically-based charging algorithms which include the effects of E-fields on atmospheric conductivity and account for the adsorption of ions and electrons onto particulates. Forward et al. conducted experiments to measure the triboelectric charging of Martian regolith simulant (JSC-1 Mars).

Summary: We have enabled our Mars regional scale atmospheric model (MRAMS) to estimate an upper limit on electric fields generated by dust devil circulations by including charged particles as defined by the Macroscopic Triboelectric Simulation (MTS) code. Our MRAMS grid cell size makes our results most applicable to dust devils of a few hundred meters in diameter. We have run a number of simulations to understand the sensitivity of the electric field strength to the particle size and abundance and the amount of charge on each dust grain. We find that E-fields can indeed develop in Martian dust convective features via dust grain filtration effects. The overall value of these E-fields is strongly dependent upon dust grain size, dust load, and lifting efficiency.

References:

Armstrong, J. C. and Leovy, C. B. (2005) "Long term wind erosion on Mars" Icarus 176, 57-74.

Barth, E.L. W.M. Farrell, S.C.R. Rafkin 2016. Electric field generation in Martian dust devils. Icarus, 268, p. 253-265.

Desch, S. J. and Cuzzi, J. N. (2000) "The Generation of Lightning in the Solar Nebula" Icarus 143, 87-105.

Farrell, W. M. et al. (2003) "A simple electrodynamic model of a dust devil" Geophysical Research Letters 30, 2050.

Farrell, W. M. et al., 2004. Electric and magnetic signatures of dust devils from the 2000-2001 MATADOR desert tests. J. Geophys. Res. 109, E03004.

Farrell, W. M. et al. (2006) "A model of the ULF magnetic and electric field generated from a dust devil" Journal of Geophysical Research 111, E11004

Fenton, L. K. and Michaels, T. I. (2010) "Characterizing the sensitivity of daytime turbulent activity on Mars with the MRAMS LES: Early results" International Journal of Mars Science and Exploration, vol. 4, p.159-171.

Forward, K.M. et al. (2009) " Particle-size dependent bipolar charging of Martian regolith simulant" Geophysical Research Letters 36, L13201.

Krauss, C. E. et al. (2003) "Experimental evidence for electrostatic discharging of dust near the surface of Mars" New Journal of Physics, Volume 5, Issue 1, 70.

Kok, J. F. and Renno, N. O. (2009) "Electrification of windblown sand on Mars and its implications for atmospheric chemistry" Geophysical Research Letters 36, L05202.

Melnik, O. and Parrot, M. (1998) "Electrostatic dis-

charge in Martian dust storms" Journal of Geophysical Research 103, 29107-29118.
Michaels, T. I. and S. C. R. Rafkin (2004) “Large eddy simulation of the convective boundary layer of Mars” Quarterly Journal of the Royal Meteorological Society 130, 1251-1274.
Michaels, T. I. (2006) "Numerical modeling of Mars dust devils: Albedo track generation" Geophysical Research Letters 33, L19S08.
Rafkin, S. C. R. et al. (2001) "The Mars Regional Atmospheric Modeling System: Model Description and Selected Simulations" Icarus 151, 228-256.
Renno, N. O. et al., 2004. MATADOR 2002: A pilot field experiment on convective plumes and dust devils. J. Geophys. Res. 109, E07001.
Sternovsky, Z. et al. (2002) "Contact charging of lunar and Martian dust simulants" Journal of Geophysical Research 107, 5105.

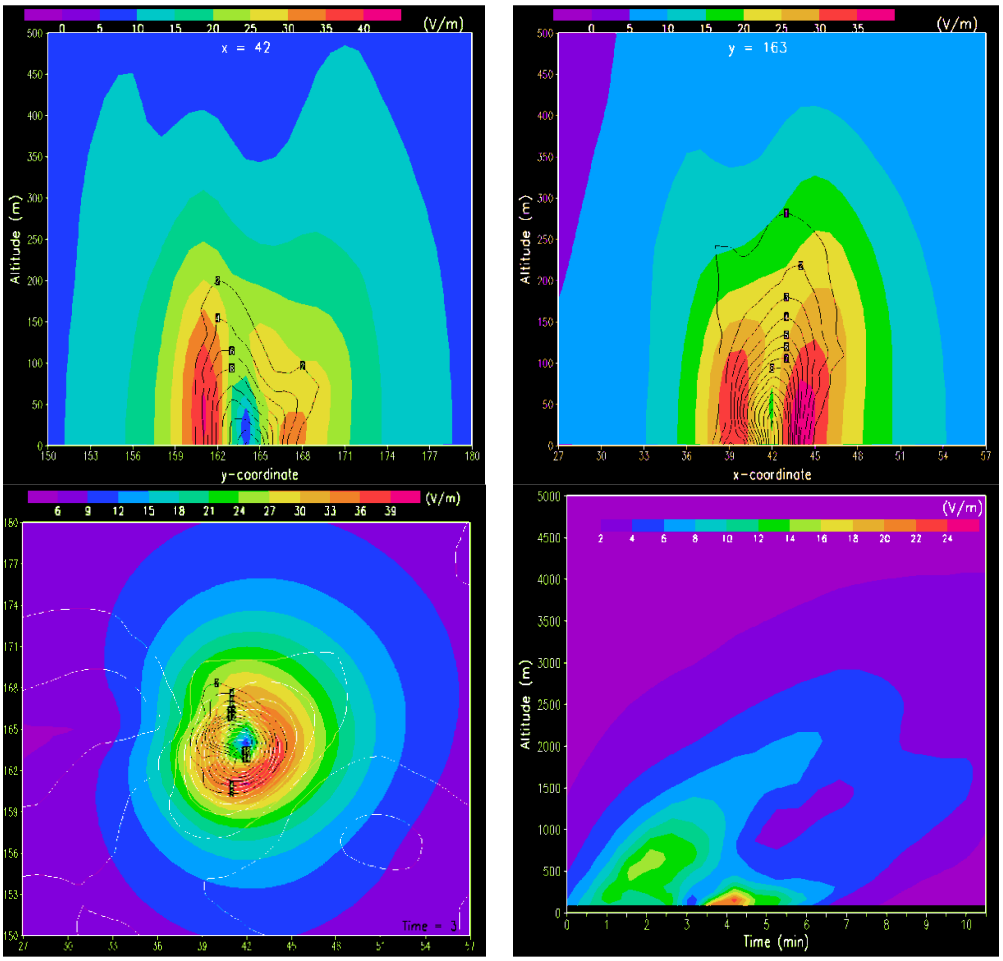

Figure 3. Electric field magnitude (colored contours) in the vicinity of a dust devil. The top row plots show vertical slices through the dust devil; black contours show number density of dust particles (#/cm^3). The bottom left plot shows a view of the dust devil in the xy-plane just above the surface, over an area of 1 km x 1 km; white pressure contours are also shown. The bottom right plot shows the temporal and vertical variation of the magnitude of the electric field (V/m) within the dust devil ; the E-field values shown here are what an observer moving with the dust devil at the minimum pressure point would see over the lifetime of the dust devil.